

# Climatological and UV-based Habitability of Possible Exomoons in F-star Systems

S. Sato<sup>1</sup>, Zh. Wang,

and

M. Cuntz<sup>2</sup>

*Department of Physics, University of Texas at Arlington,  
Arlington, TX 76019, USA*

satoko.sato@mavs.uta.edu; zhaopeng.wang@mavs.uta.edu; cuntz@uta.edu

## ABSTRACT

We explore the astrobiological significance of F-type stars of spectral type between F5 V and F9.5 V, which possess Jupiter-type planets within or close to their climatological habitable zones. These planets, or at least a subset of those, may also possess rocky exomoons, which potentially offer habitable environments. Our work considers eight selected systems. The Jupiter-type planets in these systems are in notably differing orbits with eccentricities between 0.08 (about Mars) and 0.72. We consider the stellar UV environments provided by the photospheric stellar radiation, which allows us to compute the UV habitable zones for the systems. Following previous studies, DNA is taken as a proxy for carbon-based macromolecules following the paradigm that extraterrestrial biology might be based on hydrocarbons. We found that the damage inflicted on DNA is notably different for the range of systems studied, and also varies according to the orbit of the Jupiter-type planet, especially for systems of high ellipticity, as expected. For some systems excessive values of damage are attained compared to today's Earth or during the Archean eon. Considering that the detection of exomoons around different types of stars will remain challenging in the foreseeable future, we view our work also as an example and template for investigating the combined requirements of climatological and UV-based habitability for exosolar objects.

*Subject headings:* astrobiology — celestial mechanics — planetary systems — stars: late-type

---

<sup>1</sup>Present address: Life Science Center of Tsukuba Advanced Research Alliance, University of Tsukuba, Ibaraki, 305-8577, Japan

<sup>2</sup>Corresponding author

## 1. Introduction

The identification of habitable regions around main-sequence stars constitutes a vital topic of contemporaneous astrobiological research. However, previous efforts concern mostly late-type stars at the lower end of the effective temperature scale (e.g., Lammer et al. 2013a), though notable exceptions include the work on F-type stars by Cockell (1999) and Buccino, Lemarchand & Mauas (2006). Cockell (1999) studied UV radiation environments for various main-sequence stars for different types of planetary atmospheres with different concentrations of  $N_2$  and  $CO_2$ , including genuine efforts to resemble the Archean Earth. He concluded that life may be able to survive in the vicinity of most main-sequence stars of spectral type F, G and K. Moreover, Buccino, Lemarchand & Mauas (2006) introduced the concept of a UV habitable zone (UV-HZ) for main-sequence stars, including applications to exosolar systems known at the time of study.

A more recent contribution has been made by Sato et al. (2014), henceforth called Paper I. They focused on F-type stars of masses between 1.2 and 1.5  $M_\odot$ , and considered numerous important aspects, including (1) the role of stellar main-sequence evolution, (2) the location of planets within or relative to the circumstellar habitable zones, and (3) the general influence of planetary atmospheric attenuation, which was described through parameterized attenuation functions. It was found that the damage inflicted on DNA for planets at Earth-equivalent (i.e., homeothermic) positions is between a factor of 2.5 and 7.1 higher than for solar-like stars, and the amount of damage critically depends on the planetary position. Additionally, there are intricate astrobiological relations for the time-dependency of damage during stellar evolutionary patterns. If atmospheric attenuation is considered, lesser amounts of damage are obtained in response to the model-dependent attenuation parameters. Previous work by, e.g., Cockell (1999) suggests that UV radiation has a momentous potential of inducing significant damage on (or loss of) hydrocarbon-based life forms, the fundamental question, i.e., “Is UV a friend or a foe?”, however, still remains unanswered. Favorable assessments about the role of UV, also encompassing the origin of life, stem from numerous studies, as, e.g., the work by Mulkidjanian, Cherepanov & Galperin (2003). This study indicates that UV light may have played a key role in the accumulation of the first polynucleotides through their abiogenic selection as the most UV-resistant biopolymers, a crucial step for the origin of self-replicating RNA-type molecules showing sufficient complexity for undergoing Darwinian evolution.

Setting those fundamental topics aside, noting that they are outside the main scope of our study, we tend to our main theme, which is the assessment of the UV environments of F-type stars. Objects of interest in such environments include potentially habitable ob-

jects such as Earth-type planets located in the stellar climatological habitable zone<sup>3</sup> (CLI-HZ). Other possibilities for the facilitation of habitability include objects associated with Jupiter-type planets, located in the CLI-HZ, such exosolar Trojan planets (e.g., Dvorak et al. 2004) or massive exomoons (e.g., Williams, Kasting & Wade 1997). Systems with giant planets located inside or crossing into the CLI-HZ during their orbital motion are typically unable of hosting habitable planets; see, e.g., Noble, Musielak & Cuntz (2002) and Yeager, Eberle & Cuntz (2011) for results from orbital stability simulations.

Hence, the focus of the present work is on the study of potential exomoons in the environments of F-type stars possessing observed Jupiter-type planets. The systems selected for our study include HD 8673, HD 169830, HD 33564, *v* And, HD 86264, HD 25171, 30 Ari, and HD 153950 (see Fig. 1 and Table 1) based on data sets not considering additions due to the *Kepler* mission. Figure 1 conveys the stellar positions in the HR Diagram, indicating that three stars, i.e., HD 33564, HD 25171, and 30 Ari B, are in essence zero-age main-sequence (ZAMS) stars, whereas the other five stars have started to evolve away from the main-sequence. Note that the *Kepler* mission has revealed many new systems of F-stars hosting Jupiter-type planets, constituting relevant targets of future research.

Exomoons, albeit the lack of heretofore detections have been the topic of numerous previous studies; see, e.g., Heller et al. (2014) for a recent review on the formation, prospects of habitability and detection methodologies for exomoons. Thus, the continued investigation of exomoons is timely. The topic of this work is a balanced consideration of the CLI-HZ and UV-HZ for possible exomoons in F-star systems, with consideration of Hill stability. To the best of our knowledge, no such paper has previously been published along those lines. It is structured as follows: In Sect. 2, we describe the theoretical approach, including the key equations and concepts. In Sect. 3, we introduce our target star–planet systems. In Sect. 4, we address various studies of exomoons, including the calculation of the Hill’s spheres for the exoplanets. In Sect. 5, we present the results of our study. Our summary and conclusions are given in Sect. 6.

---

<sup>3</sup>The definition of the CLI-HZ follows the work by Kasting, Whitmire & Reynolds (1993), which assumes an Earth-like planet with a CO<sub>2</sub>/H<sub>2</sub>O/N<sub>2</sub> atmosphere and that habitability requires the presence of liquid water on the object’s surface; see Sect. 2.1 for details, including updates by Kopparapu et al. (2013, 2014).

## 2. Theoretical approach

### 2.1. Climatological habitable zones

A crucial aspect in the study of circumstellar habitability is the introduction of the CLI-HZ, a concept, previously considered by Kasting, Whitmire & Reynolds (1993) and others. Even though the centerpiece of our study is quantifying impact of UV (see Sect. 2.2), the CLI-HZ is important for two reasons. First, it conveys reference distances of habitability, which can be compared to the orbits of the Jupiter-type planets. Those limits are also relevant to possible exomoons, which are expected to be in close proximity to their host planets. Second, the inner and outer limits of the CLI-HZ can also be used as markers for the assessment of UV habitability, particularly the quantity  $E_{\text{eff}}$  (see Sect. 5.1), thus allowing to interpret our results.

Previously, Kasting, Whitmire & Reynolds (1993) utilized 1-D climate models, which were state-of-the-art at the time, to estimate the position and width of the CLI-HZ for a range of main-sequence stars, include the Sun. The basic premise was the assumption of an Earth-like planet with a  $\text{CO}_2/\text{H}_2\text{O}/\text{N}_2$  atmosphere and, furthermore, that habitability requires the presence of liquid water on the object’s surface. This work was significantly updated through subsequent studies, including the work by Kopparapu et al. (2013, 2014). For example, it considers the recent Venus / early Mars (RVEM) limits of the CLI-HZ, previously considered by Kasting, Whitmire & Reynolds (1993).

Other important limits for the CLI-HZs are based on the runaway greenhouse effect (inner limit) and maximum greenhouse effect (outer limit); in the following, these limits are used to signify the general habitable zone (GHZ); see Fig. 2. As described by, e.g., Underwood, Jones & Sleep (2003), at the inner limit, the greenhouse phenomenon is enhanced by water vapor, thus promoting surface warming, which increases the atmospheric water vapor content, thus further raising the surface temperature. At sufficient stellar flux, this will trigger the rapid evaporation of all surface water. Thus, all water will be lost from the surface, and the water will also be lost from the upper atmosphere by photodissociation and subsequent water escape to space. Concerning the outer limit, it is assumed that a cloud-free  $\text{CO}_2$  atmosphere shall still be able to provide a surface temperature of 273 K. The most extreme outer limit is that for the extended habitable zone (EHZ), which in the solar system extends up to 2.40 AU (Mischna et al. 2000).

For solar-like stars, and assuming an Earth-mass object, Kopparapu et al. (2013, 2014) identified those limits as approximately 0.95 and 1.68 AU, respectively. In contrast, Kasting, Whitmire & Reynolds (1993) identified these values as 0.84 and 1.67 AU, respectively. Another important limit on habitability is given by the moist greenhouse limit, which for solar-like stars has been

updated to 0.99 AU. In the previous work by Kasting, Whitmire & Reynolds (1993) another limit was identified given by the first CO<sub>2</sub> condensation obtained by the onset of formation of CO<sub>2</sub> clouds at a temperature of 273 K, which was however not revisited by Kopparapu et al. (2013, 2014). Nevertheless, in the present work, the moist greenhouse limit and the limit due to the first CO<sub>2</sub> condensation are used to define the conservative habitable zone (CHZ), as motivated by a large array of previous studies<sup>4</sup>.

The extents of the CHZ, GHZ and EHZ for the target stars (see Table 1) are given in Table 2. The results are in agreement with previous studies, which showed that the more luminous the star, the larger the extent of the CLI-HZs. Even though the CLI-HZs of F-type stars are considerably wider than those of solar-like stars, stars with masses larger than 1.2  $M_{\odot}$  possess continuously habitable zones for less than the current age of Earth (e.g., Rushby et al. 2013; Sato et al. 2014; Cuntz & Guinan 2016). Nevertheless, this window of time may still be sufficient for the build-up of extraterrestrial biospheres. Furthermore, a higher stellar luminosity also means that the inner limits of the respective HZ is placed further outward.

A more thorough assessment of both the widths and the limits of the various types of HZs requires the consideration of both the luminosities and the effective temperatures of the target stars, which is done as part of our approach<sup>5</sup>. For example, it is found that CLI-HZ of the largest width is obtained for HD 86264, where the EHZ extends from 1.60 to 5.06 AU. Somewhat smaller extents for the CLI-HZ are found for HD 8673 and  $\nu$  And A; here the outer limits of the EHZs are given as 4.37 and 4.39 AU, respectively. Relatively small extents for the CLI-HZ are found for HD 33564 and 30 Ari B. Here the inner limits are at about 0.95 AU, whereas the outer limits extent to nearly 3.0 AU. These stars are late-type F-stars with luminosities of 1.66 and 1.64  $L_{\odot}$ , respectively (see Table 1). Figure 3 conveys the various domains of the CLI-HZs together with the exoplanetary distances from their host stars, also taking into account the eccentricities of the stellar orbits. Detailed observational results about the various target stars are the focus of Sect. 3.

---

<sup>4</sup>In the work by Kopparapu et al. (2013, 2014) the CLI-HZ given by the RVEM limits is referred to as GHZ, whereas the CLI-HZ between 0.95 and 1.68, as identified for an Earth-mass planet, is referred to as CHZ. This notation is different from that of the present study, which follows previous convention.

<sup>5</sup>Another important effect that is beyond the scope of our study is tidal heating, which is expected to affect both the inner and outer limits of the CLI-HZs as previously discussed by Barnes et al. (2008, 2013), Jackson, Barnes & Greenberg (2008), and Lammer et al. (2014), among others.

## 2.2. UV-based habitability concepts

Following Paper I, we consider the DNA action spectrum as a proxy to simulate the impact of UV radiation regarding hydrocarbon-based biostructure. Generally, an action spectrum is the rate of physiological activity plotted against wavelength or frequency of light. Biological effectiveness spectra can be derived from spectral data by multiplication with an action spectrum  $S_\lambda(\lambda)$  of a relevant photobiological reaction with the action spectrum typically given in relative units normalized to unity for, e.g.,  $\lambda = 300$  nm. The biological effectiveness for a distinct range of the electromagnetic spectrum such as UV radiation is determined by

$$E_{\text{eff}} = \int_{\lambda_1}^{\lambda_2} E_\lambda(\lambda) S_\lambda(\lambda) \alpha(\lambda) d\lambda \quad , \quad (1)$$

where  $E_\lambda(\lambda)$  denotes the stellar irradiance ( $\text{ergs cm}^{-2} \text{ s}^{-1} \text{ nm}^{-1}$ ),  $\lambda$  the wavelength (nm), and  $\alpha(\lambda)$  the planetary atmospheric attenuation function; see Horneck (1995). Here  $\lambda_1$  and  $\lambda_2$  are the limits of integration which in our computations are set as 200 nm and 400 nm, respectively. Although a significant amount of stellar radiation exists beyond 400 nm, this portion of the spectrum is disregarded in the following owing to the minuscule values for the action spectrum  $S_\lambda(\lambda)$  in this regime. Atmospheric attenuation, also referred to as extinction, results in a loss of intensity of the incident stellar radiation. In Eq. (1)  $\alpha = 1$  indicates no loss and  $\alpha = 0$  indicates a complete loss (see Sect. 2.3).

For the computation of the stellar irradiance for targets in circumstellar environments, typically positioned in the CLI-HZ (see Table 2), the domain of interest in the present study, a further equation is needed, which is

$$E_\lambda(\lambda) \propto F_\lambda(R_*/d)^2 \quad . \quad (2)$$

Here  $F_\lambda$  denotes the stellar radiative flux per unit surface,  $R_*$  is the stellar radius and  $d$  is the distance between the target and the star. Note that Eq. (2) describes the geometrical dilution of the stellar radiation field. Based on previous work, the UV region of the electromagnetic spectrum has been divided into three bands termed UV-A, UV-B, and UV-C. The subdivisions are somewhat arbitrary and differ slightly depending on the discipline involved. In Paper I, we used UV-A, 400-320 nm; UV-B, 320-290 nm; and UV-C, 290-200 nm. Due to the shape of the action spectrum, it was found that in the environments of F-type stars, most of the damage occurs with respect to UV-C. If the incident stellar radiation is largely blocked in the short wavelength regime of the DNA action spectrum, due to atmospheric attenuation (see below), the majority of damage may occur regarding UV-B. Detailed information for sets of F-type stars, also considering effects of stellar evolution, has been described in detail in Paper I.

Through using an earlier version for the DNA action spectrum previous results were given by Cockell (1999). Action spectra for DNA, also to be viewed as weighting functions, have previously been utilized to quantify damage due to UV radiation (Setlow 1974). As discussed in Paper I, the DNA action spectrum increases by almost four orders of magnitude between 400 and 300 nm (see Fig. 4). The reason for this behavior is the wavelength dependence of the absorption and ionization potential of UV radiation in this particular regime. A further significant increase in the DNA action spectrum occurs between 300 and 200 nm. Regarding Earth, it is found that the terrestrial Earth’s ozone layer is able to filter out this type of lethal radiation (e.g., Diffey 1991; Cockell 1998); the terrestrial ozone layer itself has been an important feature for allowing its oxygen level to rise, and thus paving the way for the development of more sophisticated life forms.

### 2.3. Stellar irradiance

The treatment of the stellar irradiance follows closely the concept of Paper I. The accurate account of stellar radiation is employed, including the adequate spectral energy distribution, by utilizing photospheric models computed by the PHOENIX code following; see Hauschildt (1992) and subsequent work. The adopted range of models for the F-type stars are in response to effective temperatures of 6440 K for spectral type F5, 6200 K for F8, and 6050 K for G0  $\equiv$  F10. Contrary to Paper I, early-type F stars are not part of the sample, and their spectral information is thus not needed. For stars intermediate to that grid, spectral information is interpolated in accord to the stellar effective temperatures. The PHOENIX code solves the equation of state, including a very large number of atoms, ions, and molecules. With respect to radiation, the one-dimensional spherically symmetrical radiative transfer equation for expanding atmospheres is solved, including a treatment of special relativity. Opacities are sampled dynamically over about 80 million lines from atomic transitions and billions of molecular lines, in addition to background (i.e., continuous) opacities, to provide an emerging spectral flux as reliable and realistic as possible; see Paper I for further details and references.

Figure 5 depicts the DNA response to stellar photospheric radiation in the UV range for selected stellar types between F5 and G2. The irradiance has been based on PHOENIX models using smoothing based on a bandpass of 1 nm. Next, the DNA action spectrum has been multiplied with the smoothed irradiance data for the range between 200 and 400 nm to attain the data for the figure. A relevant ingredient to our study is the consideration of atmospheric attenuation  $\alpha(\lambda)$ , which typically results in a notable reduction of the incident stellar radiation. Appropriate values for  $\alpha(\lambda)$  can be obtained through the analysis of the-

oretical exoatmospheric models (e.g., Seager & Deming 2010, and subsequent work) or the usage of model-dependent historic Earth data (e.g., Cockell 2002). Within the scope of the present work that is focused on the impact of photospheric radiation from different F-type stars, we consider  $\alpha(\lambda)$  as described by a parameterized attenuation function ATT defined<sup>6</sup> as

$$\text{ATT}(\lambda) = \frac{C}{2} \left[ 1 + \tanh(A(\lambda - B)) \right] . \quad (3)$$

Here  $A$  denotes the start-of-slope parameter,  $B$  (in nm) the center parameter, and  $C$  the maximum (limited to unity) of the distribution; see Fig. 6 and Paper I for examples of  $\text{ATT}(\lambda)$ .

For example, Cockell (2002) provided information about the ultraviolet irradiance reaching the surface of Archean Earth for various assumptions about Earth’s atmospheric composition; the latter allow us to constrain the wavelength-dependent attenuation coefficients. This particular case is akin to the choice of  $(A, B, C) = (0.02, 250, 0.5)$ . Detailed results for planetary atmospheres for the build-up and destruction of ozone have been given by, e.g., Segura et al. (2003).

## 2.4. UV habitable zones

The concept of UV habitable zones, as considered in our study, closely follows the previous work by Buccino, Lemarchand & Mauas (2006). It again follows the key idea that, on the one hand, UV radiation may have provided an important energy source for early Earth for the synthesis of many biochemical compounds and thus fostering various biogenesis processes, but, on the other hand, excessive amounts of UV are destructive (see Sect. 1). Another consideration includes the “Principle of Mediocrity” (PoM), which suggests that the biological system of Earth is about average, and that the development of life and intelligence outside of Earth is governed by the same laws and concepts as previously on Earth if proper conditions are met; see Buccino, Lemarchand & Mauas (2006) for additional comments and references. As an example of exobiology, Franck, von Bloh & Bounama (2007) employed the PoM to estimate the maximum number of habitable planets at the time of Earth’s origin in the framework of geobiology.

Akin to Eq. (1), Buccino, Lemarchand & Mauas (2006) introduced a measure for the DNA damage due to UV photons radiated by a star of age  $t$  that reaches the top of a

---

<sup>6</sup>ATT equal to 0 and 1 indicate the presence and absence of atmospheric attenuation, respectively; hence, the headers of Fig. 8 and 11 of Paper I have been mislabelled and should read  $\text{ATT} = 1$  instead.



planetary or exomoon atmosphere at a distance  $d$  (in AU). It is expressed as

$$N_{\text{DNA}}^*(d) = \int_{\lambda_1}^{\lambda_2} S_{\lambda}(\lambda) \frac{\lambda}{hc} \frac{\tilde{F}(t)(\lambda)}{d^2} d\lambda, \quad (4)$$

where  $S_{\lambda}(\lambda)$  denotes the DNA action spectrum (see Eq. 1),  $\tilde{F}$  the stellar UV flux at 1 AU,  $h$  the Planck constant, and  $c$  is the speed of light. Here we use  $\lambda_1 = 200$  nm and  $\lambda_2 = 400$  nm, although the choice of 315 nm for  $\lambda_2$ , as done by Buccino, Lemarchand & Mauas (2006), is acceptable owing to the minuscule values for  $S_{\lambda}(\lambda)$  in the UV-A regime. For  $\tilde{F}$ , the PHOENIX models are adopted, which are interpolated based on the stellar effective temperature, as needed.

The domains of the stellar UV-HZs are defined based on the PoM according to

$$N_{\text{DNA}}^*(d) = \eta N_{\text{DNA}}^{\odot}(1 \text{ AU})|_{t=t_{\text{ArcE}}^{\odot}} \quad (5)$$

with  $0.5 \leq \eta \leq 2.0$ , where  $\eta = 0.5$  and  $\eta = 2.0$  correspond to the outer and the inner limit of a UV-HZ, respectively<sup>7</sup>. Moreover,  $N_{\text{DNA}}^{\odot}(1 \text{ AU})|_{t=t_{\text{ArcE}}^{\odot}}$  is determined based on Eq. 4, using the flux received by the Archean Earth (ArcE), i.e., about  $\sim 3.8$  Gyr ago, which is assumed equal to 75% of the present Sun’s radiation on top of Earth’s atmosphere (e.g., Kasting 1988; Cockell 1998). The limits of the UV-HZs can be calculated based on Eqs. (4) and (5) through solving for  $d$ . The UV-HZs for our target stars are depicted in Fig. 7; they are also compared to the CLI-HZs. It is found that the UV-HZs are always larger than the GHZ, but are notably smaller than the respective EHZ, in consideration of that they do not extend as far outward; see Table 2 and 3 for additional information. Note that both findings also apply to the Sun, where the UV-HZ extends from 0.71 to 1.90 AU (Buccino, Lemarchand & Mauas 2006), whereas the EHZ, as defined in the present study, extends up to 2.40 AU (Mischna et al. 2000).

### 3. Target stars and planets

Next we summarize relevant information about our selection of star–planet systems considered in the present study, which are: HD 8673, HD 169830, HD 33564,  $v$  And A, HD 86264, HD 25171, 30 Ari B, and HD 153950 (see Table 1). The systems consist of an F-type star and at least one Jupiter-type planet (see Table 4); the latter are in considerably

---

<sup>7</sup>Note that the definition of the outer limit of the UV-HZ deviates from that used by Buccino, Lemarchand & Mauas (2006), which does not include the term  $S_{\lambda}(\lambda)$ .

differing orbits with eccentricities between 0.08 and 0.72. We also comment on the relationships between the planetary orbits and the stellar CLI-HZs, subdivided into the CHZs, GHZs, and EHZs (see Sect. 3.1 and Table 2). Relevant system properties include the planetary eccentricities, which are relevant for gauging the prospective of habitability of possible exomoons.

HD 8673 is an F5 V star<sup>8</sup> of  $T_{\text{eff}} = 6413$  K (Fuhrmann 2008) with a mass of  $1.3 M_{\odot}$ . The system’s age has been estimated as 2.52 Gyr (Takeda et al. 2007). HD 8673 possesses a massive planet or brown dwarf with a minimum mass of  $14.2 M_J$  at  $a_p = 3.02$  AU (Hartmann, Guenther & Hatzes 2010). Since HD 8673b has an eccentricity of 0.723, the star–planet distance varies between 0.84 AU and 5.20 AU. Hence, the planet moves beyond both the inner and outer limits of the EHZ. It also moves beyond both limits of the UV-HZ, with the total extent of star–planet distance being about a factor of 2 larger than that of the UV-HZ.

HD 169830, an F7 V star of  $T_{\text{eff}} = 6266$  K (Nordström et al. 2004) with a mass of  $1.4 M_{\odot}$  (Fischer & Valenti 2005), is host to two planets with  $a_p = 0.81$  AU and 3.6 AU, respectively (Mayor et al. 2004). The planetary minimum masses are  $2.88$  and  $4.04 M_J$ , respectively. The orbit of HD 169830c lies completely within the EHZ, but not within the UV-HZ, whereas HD 169830b is positioned much closer to the star. The eccentricity of HD 169830c is given as 0.33. Therefore, the star–planet distance varies between 2.41 AU, the periapsis, located inside the CHZ and 4.79 AU, the apoapsis, which is at a distance situated between the outer limits of the GHZ and EHZ. The stellar age is estimated as 2.3 Gyr (Nordström et al. 2004).

HD 33564 is an F7 V star of  $T_{\text{eff}} = 6250$  K (Acke & Waelkens 2004) with a mass of  $1.25 M_{\odot}$  (Nordström et al. 2004). It is a relatively inactive star with an age of 3.0 Gyr (Nordström et al. 2004; Galland et al. 2005). The star hosts a planet with a minimum mass of  $9.1 M_J$  and a semi-major axis of 1.1 AU. The planetary orbital eccentricity is given as  $e_p = 0.34$ . Therefore, the star–planet distance varies between 0.73 and 1.47 AU, implying that this inner limit is closer to the host star than the inner limit of the EHZ as well as the inner limit of the UV-HZ, though this difference is small. Furthermore, HD 33564 has two stellar companions (Dommange & Nys 2002). However, they are probably unbound to the main star as revealed by the high differences between the proper motions of the components (Galland et al. 2005; Roell et al. 2012).

$\nu$  And is a binary system, consisting of an F8 V star of  $T_{\text{eff}} = 6212$  K,  $\nu$  And A (HD 9826), and of an M4.5 V star,  $\nu$  And B (Lowrance, Kirkpatrick & Beichman 2002;

---

<sup>8</sup>The spectral types as given have been determined based on the stellar effective temperatures. They may thus be modestly different from those conveyed by the references for the other stellar properties.

Santos, Israelian & Mayor 2004). The separation between the binary components is given as 750 AU (Lowrance, Kirkpatrick & Beichman 2002), implying that any habitable environment of  $\nu$  And A would remain unaffected by  $\nu$  And B; see, e.g., the methodological approach by Cuntz (2014, 2015) to deduce the magnitude of interdependency in binary systems. Radial velocity measurements led to the detection of four planets around  $\nu$  And A, and one of the planets, i.e.,  $\nu$  And Ad, is found to be located within  $\nu$  And A’s CLI-HZ and UV-HZ. The semi-major axes of the planets  $\nu$  And Ab, c, d, and e are given as 0.0592, 0.828, 2.51, and 5.25 AU, and their minimum masses are given as 0.69, 1.98, 4.13, and  $1.06 M_J$ , respectively (Curiel et al. 2011)<sup>9</sup>. The eccentricity of  $\nu$  And Ad is identified as 0.299 (Curiel et al. 2011), and its unprojected mass has been estimated as  $10.19 M_J$  (Barnes et al. 2011). Its periapsis is at 1.76 AU, a distance close to the inner limit of the GHZ. The planet stays inside the EHZ at its apoapsis at 3.26 AU. This system is also known for the mutual inclination between the planets c and d, which is as large as  $30^\circ$  (Barnes et al. 2011).

HD 86264 is an F8 V star of  $T_{\text{eff}} = 6210$  K with a mass of  $1.42 M_\odot$  (Fischer et al. 2009). The star possesses a planet with a minimum mass of  $7.0 M_J$  at  $a_p = 2.86$  AU, i.e., slightly beyond the outer limit of the CHZ. Since the planet has an eccentricity of  $e_p = 0.7$ , it approaches the star at about half the distance of the inner limit of the EHZ at its periapsis, and approaches the outer limit of the EHZ at its apoapsis; the corresponding distance range is between 0.86 AU and 4.86 AU. The planet also crosses the inner and outer limits of the UV-HZ. HD 86264 has an age of 2.24 Gyr, and it is moderately active (Fischer et al. 2009).

HD 25171 is an F9 V star of  $T_{\text{eff}} = 6160$  K with a mass of  $1.09 M_\odot$  (Moutou et al. 2011). It is a non-active star with an age of 4.0 Gyr. It is also host to a Jupiter-type planet with a minimum mass of  $0.95 M_J$  in a nearly circular orbit with an eccentricity of  $e_p = 0.08$ , i.e., about the value of Mars. The planet orbits the star close to the outer edge of the EHZ, and most of the planetary orbit also lies beyond the stellar UV-HZ. The planet’s semi-major axis is identified as 3.02 AU. Hence, the periapsis and apoapsis are given as 2.78 AU and 3.26 AU, respectively. The outer limit of the EHZ is identified as 3.13 AU, thus nearly coinciding with the planet’s apoapsis.

30 Ari is a triple star system, consisting of the single line spectroscopic binary, 30 Ari A (HD 16246), and the single star, 30 Ari B (HD 16232). 30 Ari A (main component) is an F3 V star of  $T_{\text{eff}} = 6668$  K, and 30 Ari B is an F9 V star of  $T_{\text{eff}} = 6152$  K (Nordström et al. 2004). The separation between 30 Ari A and B is about 1520 AU (Perryman 1997; Zombeck 2007; Guenther et al. 2009), which ensures that any habitable environment of 30 Ari A and

---

<sup>9</sup>In the work by Curiel et al. (2011),  $\nu$  And Ac and d are exchanged; however, in this study we use the notation given by the sequence of observation.

B would not interfere. 30 Ari B hosts a planet at  $a_p = 0.995$  AU. This distance is slightly farther from the star than the inner limit of the EHZ, which is at 0.947 AU. Furthermore, half of the planetary orbit is closer to the star than the inner limit of the UV-HZ. The periapsis is at 0.71 AU, but a large part of the orbit is in the CLI-HZ. The apoapsis is at 1.28 AU, located in the CHZ based on an orbital eccentricity of 0.289. The stellar mass and the minimum mass of the planet are given as  $1.11 M_\odot$  (Nordström et al. 2004) and  $9.88 M_J$  (Guenther et al. 2009), respectively. The age is estimated as 0.91 Gyr (Guenther et al. 2009), implying that it is a very young star.

HD 153950 is an F9.5 V star with an effective temperature of  $T_{\text{eff}} = 6076$  K (Moutou et al. 2009), thus representing the low temperature limit of our sample. HD 153950 is host to a planet with a minimum mass of  $2.73 M_J$  and a semi-major axis of  $a_p = 1.28$  AU. The planet’s semi-major axis corresponds to a distance about halfway between the inner limit of the EHZ and the inner limit of the GHZ. Moreover, similar to the case of 30 Ari, about half of the planetary orbit is closer to the star than the inner limit of the UV-HZ. At its apoapsis, the planet is located in the CHZ, but at the periapsis, it approaches the star as close as 0.84 AU. The eccentricity is  $e_p = 0.34$  (Moutou et al. 2009). The host star has a mass of  $1.12 M_\odot$ , and its age is estimated as 4.3 Gyr.

#### 4. Studies of exomoons

Exomoons, despite that there are no detections yet, have been the topic of numerous studies. Examples include the work by Williams, Kasting & Wade (1997), Kipping, Fossey & Campanella (2009), Kaltenegger (2010), Barnes & O’Brien (2002), Heller & Barnes (2013), Cuntz et al. (2013), Heller & Zuluaga (2013), and Heller & Pudritz (2015). They consider a large variety of aspects including orbital stability considerations, formation of exomoons around super-Jovian planets, magnetic shielding of exomoons beyond the circumplanetary habitable edge, deciphering spectral fingerprints (which could potentially lead to the detection of life), and the lower mass limit of exomoons required for retaining a substantial and long-lived atmosphere.

Strictly speaking, exomoons could also be akin to terrestrial or super-Earth planets in size and mass if orbiting a Jupiter-type planet. In this case, the existence and retention of the moon’s atmosphere is expected to be virtually guaranteed; see, e.g., Tsiraras et al. (2016) for a recent observational study. Atmospheres of large exomoons might also enjoy the benefit of magnetic protection (e.g., Lammer et al. 2003; Grießmeier et al. 2004, and subsequent work), which will be able to counteract the impact of energetic stellar radiation, especially for young stars (e.g., France, Linsky & Parke Loyd 2014; Cuntz & Guinan 2016,

and references therein). Detailed studies about atmospheric losses due to energetic stellar radiation have previously been given by Erkaev et al. (2013), Lammer et al. (2013b), and Cohen et al. (2015), among others.

Additional studies about exomoons have been devoted to search methodologies as discussed by, e.g., Awiphan & Kerins (2013), Kipping et al. (2013), Kipping (2014), Heller et al. (2014), and Noyola, Satyal & Musielak (2014). The work of Awiphan & Kerins and Kipping, including subsequent studies by the same group of authors, focused on the detectability of potentially habitable exomoons, i.e., exomoons located in the stellar CLI-HZs. Emphasis has been placed on results from the *Kepler* space mission through the virtue of photodynamics and sophisticated data analysis techniques. Noyola, Satyal & Musielak (2014) suggested to identify exomoons through observations of radio emissions; this type of research is guided by the physical structure of the Jupiter–Io system.

A crucial aspect for the existence of exomoons concerns the necessity of orbital stability. Because of three-body interaction, moons will be lost from their host planet if the distance between the planet and moon is too large. This underlying orbital stability limit cannot be calculated in a straightforward manner, see, e.g., Musielak & Quarles (2014) and references therein, although provisional insight can be obtained if assumed that the moon’s orbit must remain within the Hill sphere (or Hill radius) given as

$$R_H = a_p(1 - e_p) \left( \frac{M_p}{3M_*} \right)^{\frac{1}{3}} ; \quad (6)$$

see Barnes & O’Brien (2002) and references therein. Here  $M_p$  and  $M_*$  denote the mass of the planet and star, whereas  $a_p$  and  $e_p$  denote the semi-major axis and eccentricity of the exoplanetary orbit, respectively.

Results are given in Table 5. If the unprojected planetary mass is unavailable,  $\sin i$  is assumed as  $\pi/4$  to calculate  $M_p$ . For HD 169830c and  $v$  And Ad, the Hill radius is found as  $R_H \simeq 0.25$  AU (see Fig. 7), which allow ample space for exomoons if successfully formed. Note that the extent of the Hill radius is adversely impacted by the exoplanet’s orbital eccentricity. Therefore, for tutorial reasons, we also convey  $\tilde{R}_H$  given as  $R_H/(1 - e_p)$ . Moreover, we also list  $R_H/a_p$  to indicate the relative importance of the Hill radius for each system. In this regard, we found that the relative extent of the Hill radius is most pronounced for 30 Ari Bb, closely followed by  $v$  And Ad, and least pronounced for HD 8673b. However, though widely used, the Hill radius is a far-from-perfect measure for assessing or predicting the orbital stability of possible exomoons in those systems as typically only a moderate fraction of  $R_H$  is available. Limitations and modifications of the concept of Hill radius, also referred to as Hill stability, have been explored by, e.g., Domingos, Winter & Yokoyama (2006), Cuntz & Yeager (2009), Hinkel & Kane (2013), and others.

## 5. Results and discussion

As part of our study, we explore the impact of the UV levels that possible exomoons of the eight systems would experience by computing  $E_{\text{eff}}$  for the CLI-HZs and for the various exoplanetary orbits.  $E_{\text{eff}}$  describes the ratio of UV infliction on DNA for a particular set of conditions to the case without any atmospheric interference for an object at 1 AU from the Sun. Hence,  $E_{\text{eff}} = 1$  implies that the set of conditions creates a similar level of UV-based damage as it would be found immediately above the Earth’s atmosphere. Here we simulate the case of no atmosphere as well as four cases of different atmospheric attenuations for each planetary system.

The results of the case without atmospheric attenuation, i.e.,  $\text{ATT} = 1$ , are given in Fig. 8. The ranges of  $E_{\text{eff}}$  corresponding to the CLI-HZs and to the orbits of possible exomoons (represented by their hosts, the Jupiter-type planets) are shown by different colors. As expected, the UV levels in the CLI-HZs of the F-type stars are generally more severe than for the solar environment, except for regions beyond the outer limits of the GHZs. In the most severe case, found at the inner limit of the EHZ for HD 8673,  $E_{\text{eff}}$  is 5.2. For this star,  $E_{\text{eff}}$  at the outer limits of the GHZ and EHZ are 1.1 and 0.53, respectively. At the inner limit of the EHZ of HD 153950, which has the lowest  $T_{\text{eff}}$  of our target stars,  $E_{\text{eff}}$  is given as 3.2. For HD 153950,  $E_{\text{eff}}$  at the outer limits of the CHZ, GHZ, and EHZ are identified as 1.0, 0.63 and 0.32, respectively.

The distances between the host stars and the various limits of CLI-HZs are strongly correlated with the stellar luminosities rather than the stellar effective temperatures. However,  $E_{\text{eff}}$  at the limits of the CLI-HZs is mostly correlated with the star’s effective temperature. For example,  $E_{\text{eff}}$  at the inner limit of the EHZ for a relatively hot star is higher than that for a relatively cool star. Moreover, the differences between  $E_{\text{eff}}$  at the various outer and inner limits of a CLI-HZ are correlated with the stellar effective temperatures as well, whereas the widths of CLI-HZs mostly depend on the stellar luminosities. Thus,  $E_{\text{eff}}$  shows a steep rate of change with location within the CLI-HZ for a hot, but less luminous star.

In the case of HD 33564, the EHZ extends from 0.95 to 2.99 AU (see Table 2), and the values for the  $E_{\text{eff}}$  at the limits are given as 4.7 and 0.47, respectively. In contrast, HD 86264, which is cooler but more luminous than HD 33564, has a wider EHZ extending from 1.60 to 5.06 AU; thus, the change in  $E_{\text{eff}}$  with distance in the CLI-HZ is more gradual. For HD 86264,  $E_{\text{eff}}$  at the inner and outer limit of the EHZ is identified as 4.5 and 0.45, respectively. However, a wider CLI-HZ does not necessarily imply that there is a wider area of a relatively mild UV environment. For example, the EHZ of HD 8673 extends from 1.39 to 4.37 AU, but the region in the EHZ with  $E_{\text{eff}} \leq 1$  only extends from 3.17 to 4.37 AU. HD 15395 has a narrower EHZ, extending from 1.10 to 3.48 AU, but has a slightly wider

region within the EHZ with  $E_{\text{eff}} \leq 1$ ; this latter region extends from 1.96 to 3.48 AU. Also note that for any star considered in our study, the  $E_{\text{eff}}$  values obtained at the outer limits of the EHZs are fairly similar.

The UV environments along the orbits of possible exomoons, hosted by exoplanets of very high eccentricities, i.e., HD 8673b and HD 86264b (see Table 4), are most severe, as expected. Hypothetical exomoons of HD 8673b and HD 86264b would experience  $E_{\text{eff}}$  values as high as 14.3 and 15.7, respectively, at the periapsis; however, these values would decrease to 0.37 and 0.49, respectively, at the exoplanets’ apoapsis positions. Fortunately, following Kepler’s second law, excursions of these exoplanets, and by implication, any possible exomoon, close to the host stars would be only of relatively short durations considering the relatively high orbital speeds at those positions. In contrast, HD 25171b’s orbit has a relatively low eccentricity, entailing that any possible exomoon would face an environment even milder than that of today’s Earth. Furthermore, any possible exomoon would be subjected to small fluctuations regarding possible DNA damage along its orbit, ranging from  $E_{\text{eff}} = 0.38$  to 0.52. The UV environments for HD 196830c and  $\nu$  And Ad are relatively moderate as well. The values of  $E_{\text{eff}}$  at the periapsis and apoapsis of HD 196830c are identified as 2.1 and 0.52, whereas for  $\nu$  And Ad, they are given as 2.8 and 0.82, respectively.

We also studied the impact of atmospheric attenuation regarding UV habitability of possible exomoons. It is found that  $E_{\text{eff}}$  is greatly reduced for the four cases of atmospheric attenuation taken into account, with the combinations of attenuation parameters given as (i)  $(A, B, C) = (0.02, 250, 0.5)$ , (ii)  $(0.05, 250, 0.5)$ , (iii)  $(0.02, 300, 0.5)$ , and (iv)  $(0.05, 300, 0.5)$  (see also Paper I). Case (iv) attenuates UV radiation most effectively. Case (ii) is the least effective of the four cases. In Case (iv),  $E_{\text{eff}}$  in the CLI-HZs is almost at the same level for all systems taken into account. Note that case (i) approximately corresponds to the atmospheric setting of the Archean Earth that has been realized about  $\sim 3.8$  Gyr ago.

Regarding HD 8673,  $E_{\text{eff}}$  is given as 0.17 and 0.018 at the inner and outer limits of the EHZ, respectively. Similarly, the values for the  $E_{\text{eff}}$  at the inner and outer limits of the EHZ of HD 153950 are given as 0.13 and 0.013, respectively. Even Case (ii) shows a drastic reduction in  $E_{\text{eff}}$  compared to the case without atmospheric attenuation. In this case,  $E_{\text{eff}}$  is given as 1.5 and 0.15 at the inner and outer limits of the EHZ of HD 8673, respectively. Moreover,  $E_{\text{eff}}$  is found as 1.0 and 0.10 at the inner and outer limit of the EHZ of HD 153950, respectively. The effect of atmospheric attenuation is highly significant in extreme situations for possible exomoons, as, e.g., at the periapsis position of HD 86264b.  $E_{\text{eff}}$  in that case is reduced to (i) 4.5, (ii) 4.9, (iii) 1.6, and (iv) 0.6. On the other hand,  $E_{\text{eff}}$  at the apoapsis position of HD 86264b is given as (i) 0.14, (ii) 0.15, (iii) 0.049, and (iv) 0.019. Concerning possible exomoons of HD 25171b, atmospheric attenuation as assumed results

in even gentler UV environments. At the periapsis and apoapsis positions of HD 257171b,  $E_{\text{eff}}$  is given as (i) 0.15 and 0.10, (ii) 0.16 and 0.12, (iii) 0.052 and 0.038, and (iv) 0.020 and 0.015, respectively. Again, the case (i) is aligned to the atmospheric attenuation of the Archean Earth.

## 6. Summary and conclusions

The aim of this study is to provide a tentative exploration of the astrobiological significance of selected F-type stars based on their UV environments, which host Jupiter-type planets within or close to their CLI-HZs; it is assumed that these planets may also be hosts to exomoons. In this context, we pursue a balanced consideration of the CLI-HZ and UV-HZ for those systems, with the orbital stability of the possible exomoons described by the Hill stability criterion as well as by the work of Domingos, Winter & Yokoyama (2006). The planets have different orbital properties, noting that their semi-major axes range from 0.995 to 3.02 AU, and the eccentricities range from 0.08 (almost circular) to 0.72 (highly elliptical). Furthermore, the host stars have notably different masses and ages. The youngest star is 30 Ari B, an early main-sequence star, with an age of  $0.91 \pm 0.3$  Gyr (Guenther et al. 2009). The most advanced stars are HD 25171 and HD 153950 with ages of  $4.0 \pm 1.6$  Gyr (Moutou et al. 2011) and  $4.3 \pm 1.0$  Gyr (Moutou et al. 2009). Although exomoons have not yet been detected for systems, the possible existence of moons stems from inspecting the Solar System, noting that Jupiter and Saturn possess two to five planet-like moons combined, with the exact number dependent on the adopted standard. Generally, even if exomoons turn out to be absent in our systems of study, our approach will offer a template for tentatively assessing habitability in other systems with exomoons, if identified.

We recognize that the discovery of exomoons in F-star systems is particularly challenging; in fact, from the current point-of-view it is beyond existing technology. Generally, observational constraints on the atmospheres of exoplanets might be accessible through stellar transits (Kaltenegger 2010). In case of exomoons, a hypothetical opportunity might exist through exomoon transits around luminous, directly imaged giant planets (Heller & Albrecht 2014). On the other hand, exomoon detections around F-type stars will be particularly challenging (and reserved to future endeavors) because of the tiny moon-to-star radius ratio (Sartoretti & Schneider 1999; Simon, Szatmáry & Szabó 2007; Heller 2014). Thus, the value of our study should be considered in a more general context, as it constitutes a particular theoretical example of (potential) habitability of exomoons, which we intend to augment to other cases, including giant planets around stars of later spectral types, which are transitting.

Our approach includes the calculation of updated sizes for the CLI-HZs following work



by Kopparapu et al. (2013, 2014), and most importantly, the role of UV due to the stellar photospheric radiation based on the approach of Paper I. Additionally, we explore the UV-HZ for the various systems, previously introduced by Buccino, Lemarchand & Mauas (2006), which is found to be about 1.5 times as large as the GHZ, but smaller than the EHZ as adopted here. Motivated by earlier studies, as, e.g., the work by Cockell (1999), DNA is taken as a proxy for carbon-based macromolecules following the paradigm that extraterrestrial biology may be most likely based on hydrocarbons; see, e.g., Kolb (2015). The DNA action spectrum is utilized to represent the impact of the stellar UV radiation; this allows us to assess different systems with or without the consideration of atmospheric attenuation. However, no calculation of damage is made for wavelength below 200 nm, mostly because no data for action spectra for DNA or other relevant biomolecules could be located for that regime. Even though the properties of possible exomoon atmospheres in the mid- and far-UV regime are unknown, F-star photospheres are expected to be significant emitters down to  $\sim 160$  nm or more (depending on their temperature and activity range), as previously pointed out by, e.g., France, Linsky & Parke Loyd (2014) and Cuntz & Guinan (2016).

Another import aspect concerns the impact of stellar evolution and the associated stability of the CLI-HZs; both are largely determined by the stellar mass — see Paper I for details. Most stars of our sample have masses between 1.1 and 1.3  $M_{\odot}$ . The most massive star is HD 86264 with a mass of about 1.42  $M_{\odot}$  (Fischer et al. 2009). According to Paper I, this star should be able to maintain<sup>10</sup> its CHZ and GHZ for about 2.1 and 2.9 Gyr, respectively; these values are commensurate to its age. Stars with masses of 1.1, 1.2, and 1.3  $M_{\odot}$  (the majority of our target stars) possess CHZs for timespans of 3.45, 3.1, and 2.7 Gyr, respectively, with the duration of the GHZs increased by a factor of 1.5 to 2.0.

These timescales are notably shorter than for the Sun; however, geochemical results for Earth by, e.g., Mojzsis et al. (1996) and most recently by Nutman et al. (2016) based on the analysis of microbial structures have convincingly shown that the origin of terrestrial life dates back to 3.8 Gyr (or longer), indicating that life might in principle be able to start a few hundred millions of years after the formation of the hosting object. This implies that even F-type stars should in general be able to provide habitable environments. Moreover, even for stars like HD 25171 and HD 153950, which already have left the main-sequence, the provision of biospheric environments might still be possible as planets or moons originally located outside of the CLI-HZs might subsequently be able to move in, which is consistent with the cases studied here. This possibility is known as cold-start solution for habitability, as pointed out by Kasting, Whitmire & Reynolds (1993) and others.

---

<sup>10</sup>This value is given by the preservation of the half-width of the respective CLI-HZ as both its inner and outer limit move outward due to the increase of luminosity caused by stellar main-sequence evolution.

The exomoons, if existing, are considered to be in close proximity to the Jupiter-type planets; therefore, the orbits of these planets are decisive for assessing the general prospects of habitability. The UV exposures of the exomoons vary according to the changes in the star–planet distances dictated by the ellipticity of the planetary orbits. For example, it is found that the exoplanets HD 169830c and  $\nu$  And Ad stay within the CLI-HZ at all times, if the most extended limits are assumed. Furthermore,  $\nu$  And Ad also remains in the UV-HZ all the time; however, the other exoplanets do not. Moreover, HD 8673b and HD 86264b make significant excursions beyond both the inner and outer limits of the CLI-HZ even if the most extended limits are considered. This behavior may nullify the exomoon’s potential for habitability depending on its atmospheric and geological conditions, even though limited excursions from the CLI-HZ may be permissible, especially for objects of thick atmospheres, as argued by, e.g., Williams & Pollard (2002). Furthermore, Abe et al. (2011) explored habitability of water-limited objects, sometimes referred to as land-worlds (e.g., Franck et al. 2003), and found that they could remain habitable much closer to the stars, a result relevant for the systems HD 8673, HD 33564, HD 86264, 30 Ari B, and HD 153950.

UV habitability in the context of this study has been measured by  $E_{\text{eff}}$ , defined as the ratio of damage for a given distance from the star for an object with or without atmospheric attenuation, as chosen by the model, relative to the damage for an object at 1 AU from a solar-like star without atmospheric attenuation. Inspections of our results show that for the hypothetical exomoon environments of the stars HD 8673 and HD 86264, in the absence of atmospheric attenuation, the highest values for  $E_{\text{eff}}$  are attained, given as about 14 and 15, respectively, which apply to the periapsis positions of the Jupiter-type planets. Relative decent values of 2.1 (maximum value) and 0.5 (persistent value) are found for the hypothetical exomoon environments of HD 169830 and HD 25171, respectively. All values of  $E_{\text{eff}}$ , including the exceptionally high values, are drastically reduced if atmospheric attenuation is applied, as identified for Earth, and as suggested for other objects beyond the Solar System (e.g., Segura et al. 2003).

Our study shows that the damage inflicted on DNA exhibit a large range of values compared to an Earth-type planet at Earth-equivalent (i.e., homeothermic) positions in the solar system. Typically, these values are relatively high, especially is at periapsis position. However, appropriate protection due to atmospheric attenuation can dramatically increase the chances of providing habitable environments, which indicates another strong motivation for the continuation of exoplanet and exomoon focused atmospheric investigations. Current results have been given by Seager & Deming (2010), Rugheimer et al. (2013), Madhusudhan et al. (2014), among others. Considering that the detection of exomoons around different types of stars (including G, K, and M dwarfs as well as regarding planets in transit) will remain challenging in the foreseeable future, we view our work also as a template

for future investigation of habitability. Among other criteria, the joint consideration of the stellar CLI-HZ and UV-HZ appears to be of particular importance.

This work has been supported by the Department of Physics, University of Texas at Arlington. We also appreciate comments by R. Heller on an early version of the manuscript.

## REFERENCES

- Abe, Y., Abe-Ouchi, A., Sleep, N.H. & Zahnle, K.J. 2011, *Astrobiol.* 11, 443
- Acke, B. & Waelkens, C. 2004, *A&A*427, 1009
- Awiphan, S. & Kerins, E. 2013, *MNRAS*432, 2549
- Baines, E.K., McAlister, H.A., ten Brummelaar, T.A., et al. 2008, *ApJ*680, 728
- Barnes, R., Raymond, S.N., Jackson, B. & Greenberg, R. 2008, *Astrobiol.* 8, 557
- Barnes, R., Greenberg, R., Quinn, T.R., McArthur, B.E. & Benedict, G.F. 2011, *ApJ*726, 71
- Barnes, R., Mullins, K., Goldblatt, C., Meadows, V.S., Kasting, J.F. & Heller, R. 2013, *Astrobiol.* 13, 225
- Barnes, J.W. & O’Brien, D.P. 2002, *ApJ*575, 1087
- Buccino, A.P., Lemarchand, G.A. & Mauas, P.J.D. 2006, *Icarus* 183, 491
- Cockell, C.S. 1998, *J. Theor. Biol.* 193, 717
- Cockell, C.S. 1999, *Icarus* 141, 399
- Cockell, C.S. 2002, in: G. Horneck & C. Baumstark-Khan (eds.), *Astrobiology: The quest for the conditions of life*, Springer, Berlin
- Cohen, O., Ma, Y., Drake, J.J., Glocer, A., Garraffo, C., Bell, J.M. & Gombosi, T.I. 2015, *ApJ*806, 41
- Cuntz, M. 2014, *ApJ*780, 14
- Cuntz, M. 2015, *ApJ*798, 101
- Cuntz, M. & Guinan, E.F. 2016, *ApJ*827, 79
- Cuntz, M. & Yeager, K.E. 2009, *ApJ*697, L86
- Cuntz, M., Quarles, B., Eberle, J. & Shukayr, A. 2013, *PASA* 30, e033
- Curiel, S., Cantó, J., Georgiev, L., Chávez, C.E. & Poveda, A. 2011, *A&A*525, A78
- Diffey, B.L. 1991, *Physics in Medicine and Biology* 36, 299

- Domingos, R.C., Winter, O.C. & Yokoyama, T. 2006, MNRAS373, 1227
- Dommanget, J. & Nys, O. 2002, VizieR Online Data Catalog: I/274, *Catalog of the components of double & multiple stars*, Observations et Travaux 54, 5
- Dvorak, R., Pilat-Lohinger, E., Schwarz, R. & Freistetter, F. 2004, A&A426, L37
- Erkaev, N.V., Lammer, H., Odert, P., et al. 2013, Astrobiol. 13, 1011
- Fischer, D.A. & Valenti, J. 2005, ApJ622, 1102
- Fischer, D., Driscoll, P., Isaacson, H., et al. 2009, ApJ703, 1545
- France, K., Linsky, J.L. & Parke Loyd, R.O. 2014, Ap&SS354, 3
- Franck, S., Cuntz, M., von Bloh, W. & Bounama, C. 2003, IJAsB 2, 35
- Franck, S., von Bloh, W. & Bounama, C. 2007, IJAsB 6, 153
- Fuhrmann, K., Pfeiffer, M.J. & Bernkopf, J. 1998, A&A336, 942
- Fuhrmann, K. 2008, MNRAS384, 173
- Galland, F., Lagrange, A.-M., Udry, S., et al. 2005, A&A444, L21
- Grießmeier, J.-M., Stadelmann, A., Penz, T., et al. 2004, A&A425, 753
- Guenther, E.W., Hartmann, M., Esposito, M., et al. 2009, A&A507, 1659
- Hauschildt, P.H. 1992, JQSRT 47, 433
- Hartmann, M., Guenther, E.W. & Hatzes A. P. 2010, ApJ717, 348
- Heller, R. 2014, ApJ787, 14
- Heller, R. & Albrecht, S. 2014, ApJ796, L1
- Heller, R. & Barnes, R. 2013, Astrobiol. 13, 18
- Heller, R. & Pudritz, R. 2015, ApJ806, 181
- Heller, R. & Zuluaga, J.I. 2013, ApJ776, L33
- Heller, R., Williams, D., Kipping, D., et al. 2014, Astrobiol. 14, 798
- Hinkel, N.R. & Kane, S. R. 2013, ApJ774, 27

- Horneck, G. 1995, *J. Photochem. Photobiol. B: Biology* 31, 43
- Jackson, B., Barnes, R. & Greenberg, R. 2008, *MNRAS* 391, 237
- Kaltenegger, L. 2010, *ApJ* 712, L125
- Kasting, J.F. 1988, *Icarus* 74, 472
- Kasting, J.F., Whitmire, D.P. & Reynolds, R.T. 1993, *Icarus* 101, 108
- Kipping, D.M. 2014, in *Frank N. Bash Symposium 2013: New horizons in astronomy*, arXiv:1405.1455
- Kipping, D.M., Fossey, S.J. & Campanella, G. 2009, *MNRAS* 400, 398
- Kipping, D.M., Forgan, D., Hartman, J., et al. 2013, *ApJ* 777, 134
- Kolb, V.M. 2015, (ed.) *Astrobiology. An evolutionary approach*, CRC Press, Boca Raton
- Kopparapu, R.K., Ramirez, R., Kasting, J.F., et al. 2013, *ApJ* 765, 131; Erratum 770, 82
- Kopparapu, R.K., Ramirez, R.M., SchottelKotte, J., et al. 2014, *ApJ* 787, L29
- Lammer, H., Selsis, F., Ribas, I., et al. 2003, *ApJ* 598, L121
- Lammer, H., Blanc, M., Benz, W., et al. 2013, *Astrobiol.* 13, 793
- Lammer, H., Erkaev, N.V., Odert, P., Kislyakova, K.G., Leitzinger, M. & Khodachenko, M.L. 2013, *MNRAS* 430, 1247
- Lammer, H., Schiefer, S.-C., Juvan, I., et al. 2014, *Origins of Life and Evolution of Biospheres* 44, 239
- Lowrance, P.J., Kirkpatrick, J.D. & Beichman, C.A. 2002, *ApJ* 572, L79
- Madhusudhan, N., Knutson, H., Fortney, J.J. & Barman, T. 2014, in: H. Beuther, R.S. Klessen, C.P., Dullemond, T. Henning (eds.), *Protostars and Planets VI*, Univ. of Arizona Press, Tucson, p. 739
- Mayor, M., Udry, S., Naef, D., et al. 2004, *A&A* 415, 391
- Mischna, M.A., Kasting, J.F., Pavlov, A. & Freedman, R. 2000, *Icarus* 145, 546
- Mojzsis, S.J., Arrhenius, G., McKeegan, K.D., Harrison, T.M., Nutman, A.P. & Friend, C.R.L. 1996, *Nature* 384, 55

- Moutou, C., Mayor, M., Lo Curto, G., et al. 2009, A&A496, 513
- Moutou, C., Mayor, M., Lo Curto, G., et al. 2011, A&A527, A63
- Mulkidjanian, A. Y., Cherepanov, D.A. & Galperin, M.Y. 2003, BMC Evol. Biol. 3, 12
- Musielak, Z.E. & Quarles, B.L. 2014, Rep. Progr. Phys. 77, 065901
- Noble, M., Musielak, Z.E. & Cuntz, M. 2002, ApJ572, 1024
- Nordström, B., Mayor, M., Andersen, J., et al. 2004, A&A418, 989
- Noyola, J.P., Satyal, S. & Musielak, Z. E. 2014, ApJ791, 25
- Nutman, A.P., Bennett, V.C., Friend, C.R.L., Van Kranendonk, M.J. & Chivas, A.R. 2016, Nature 537, 535
- Pasinetti Fracassini, L. E., Pastori, L., Covino, S. & Pozzi, A. 2001, A&A367, 521
- Perryman, M.A.C. 1997, *The HIPPARCOS and TYCHO Catalogues*, SP-1200, ESA, Noordwijk
- Rushby, A.J., Claire, M.W., Osborn, H. & Watson, A.J. 2013, Astrobiol. 13, 833
- Roell, T., Neuhäuser, R., Seifahrt, A. & Mugrauer, M. 2012, A&A542, A92
- Rugheimer, S., Kaltenegger, L., Zsom, A., Segura, A. & Sasselov, D. 2013, Astrobiol. 13, 251
- Santos, N.C., Israelian, G. & Mayor, M. 2004, A&A415, 1153
- Sartoretti, P. & Schneider, J. 1999, A&AS 134, 553
- Sato, S., Cuntz, M., Guerra Olvera, C.M., Jack, D. & Schröder, K.-P. 2014, IJAsB 13, 244 [Paper I]
- Seager, S. & Deming, D. 2010, ARA&A48, 631
- Segura, A., Krelove, K., Kasting, J.F., et al. 2003, Astrobiol. 3, 689
- Setlow, R.B. 1974, Proc. Natl. Acad. Sci. USA 71, 3363
- Simon, A., Sztatmáry, K. & Szabó, Gy.M. 2007, A&A470, 727
- Takeda, G., Ford, E.B., Sills, A., et al. 2007, ApJS168, 297

- Tsiaras, A., Rocchetto, M., Waldmann, I.P., et al. 2016, ApJ820, 99
- Underwood, D.R., Jones, B.W. & Sleep, P.N. 2003, IJAsB 2, 289
- Williams, D.M. & Pollard, D. 2002, IJAsB 1, 61
- Williams, D.M., Kasting, J.F. & Wade, R.A. 1997, Nature 385, 234
- Yeager, K.E., Eberle, J. & Cuntz, M. 2011, IJAsB 10, 1
- Zombeck, M.V. 2007, *Handbook of astronomy and astrophysics*, 3rd edn., Cambridge Univ. Press, New York



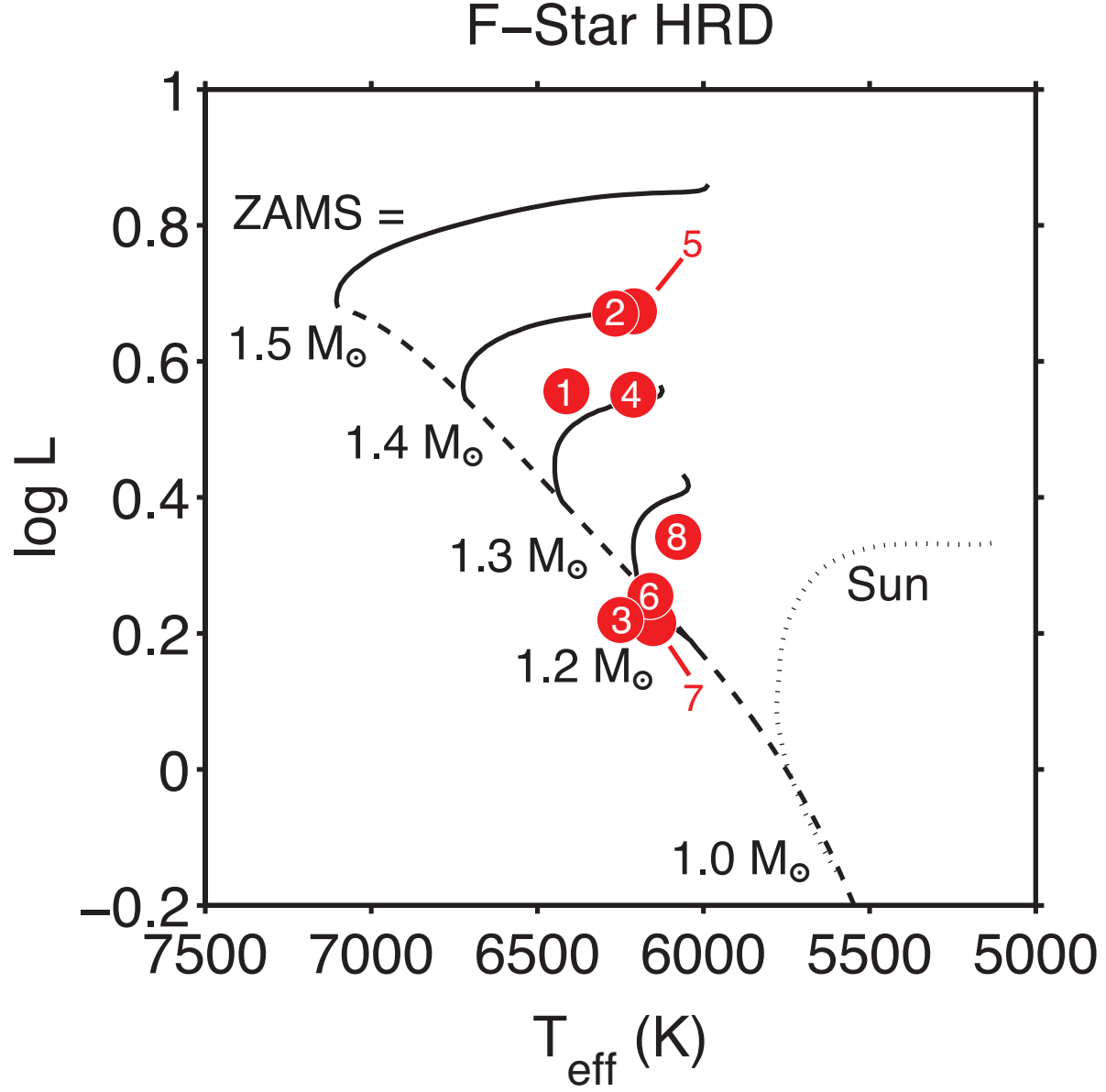


Fig. 1.— Stellar evolutionary tracks for F-type stars of different masses (solid lines) with the main-sequence depicted by a dashed line. The positions of the eight target stars (see Table 1) considered in the present study are labeled accordingly. The evolutionary track for the Sun (G2 V) is depicted as a dotted line for comparison.

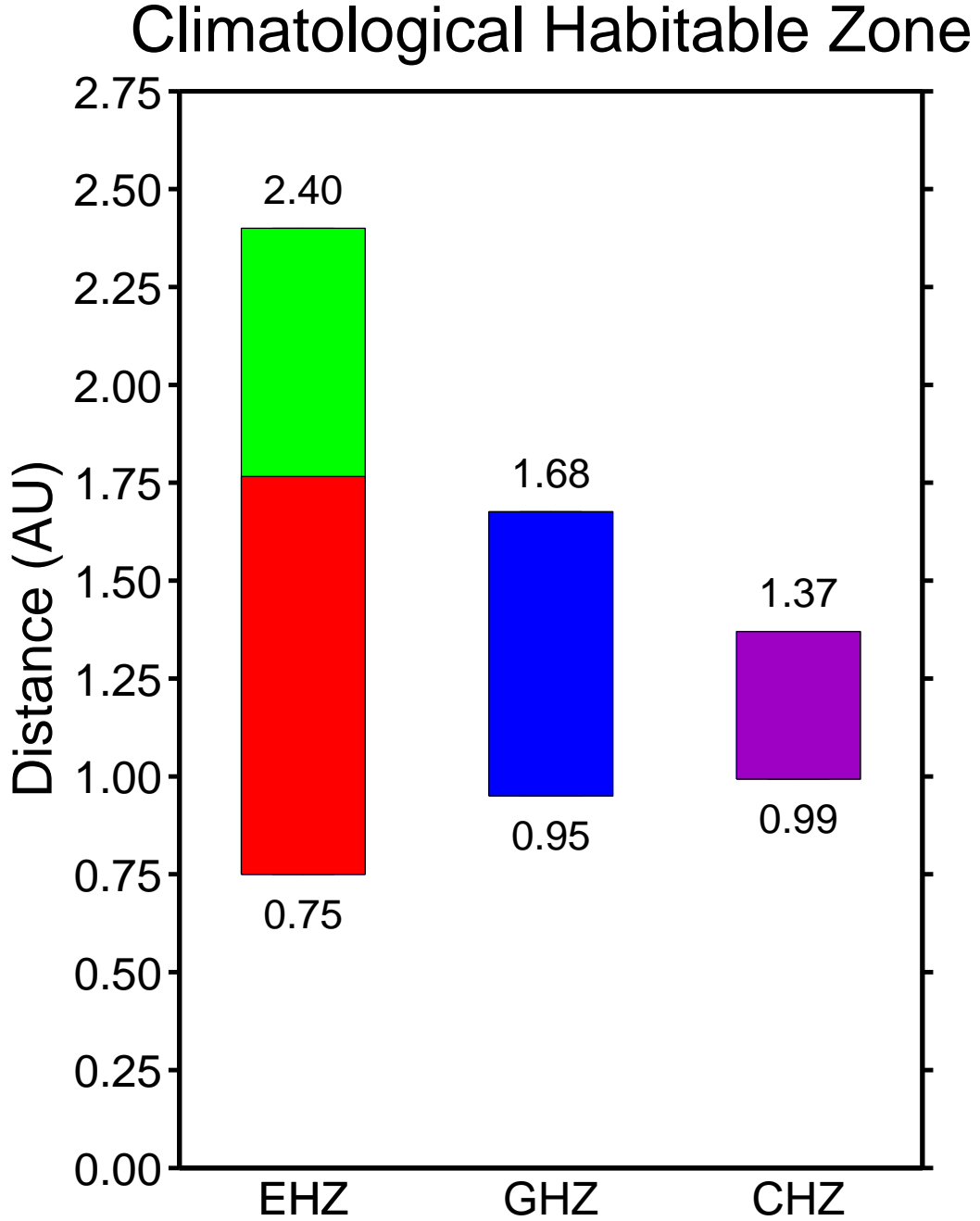


Fig. 2.— Types of CLI-HZs; the EHZ, GHZ, and CHZ are color coded. Regarding the EHZ, the range defined by the RVEM limits is depicted in red, whereas the extension based on the work by Mischna et al. (2000) is depicted in green.

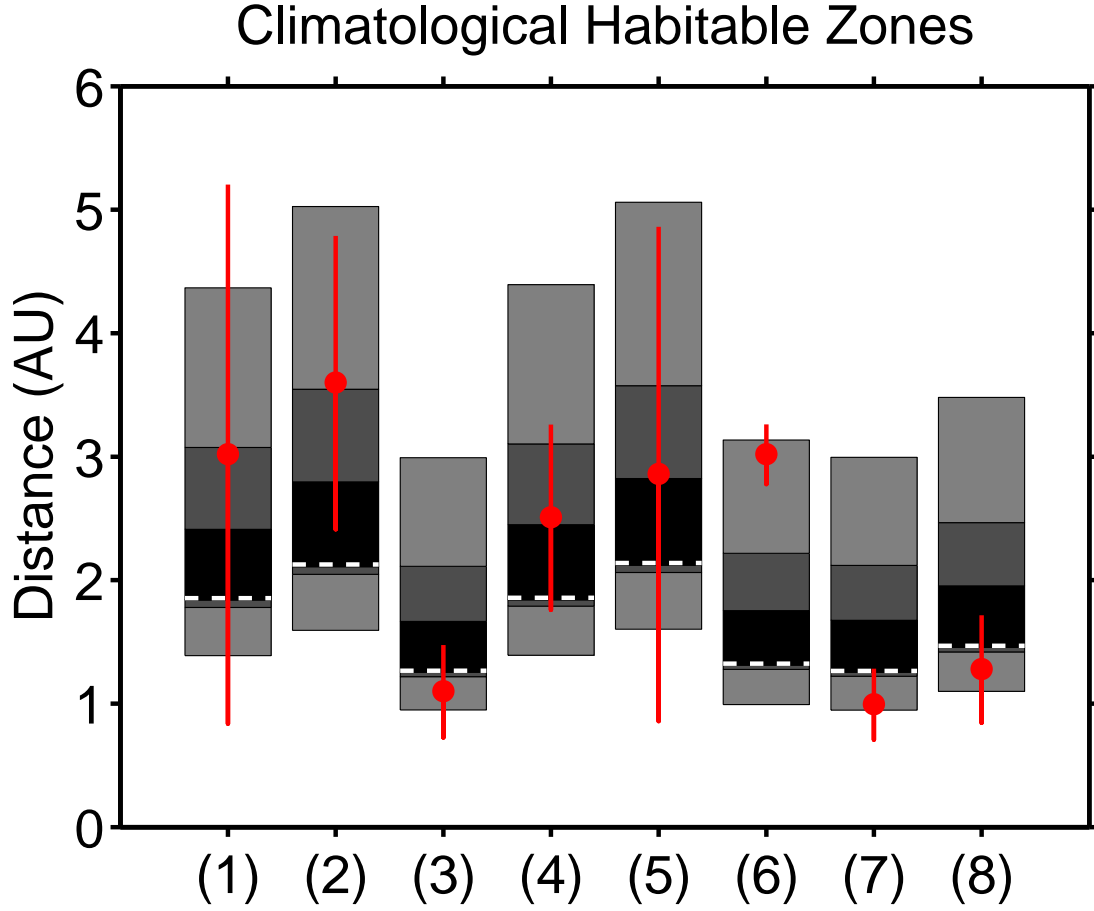


Fig. 3.— Domains of the stellar CLI-HZs, subdivided into the respective CHZs (dark gray), GHZs (medium gray), and EHZs (light gray), for the various target stars (see Table 1) indicated by (1) to (8). The Earth-equivalent positions, roughly given by the square root of the stellar luminosities, are indicated as dashed lines. The positions of the giant planets are shown as red dots, whereas the ranges of the star–planet distances due to the eccentricity of the planetary orbits are shown as red lines.

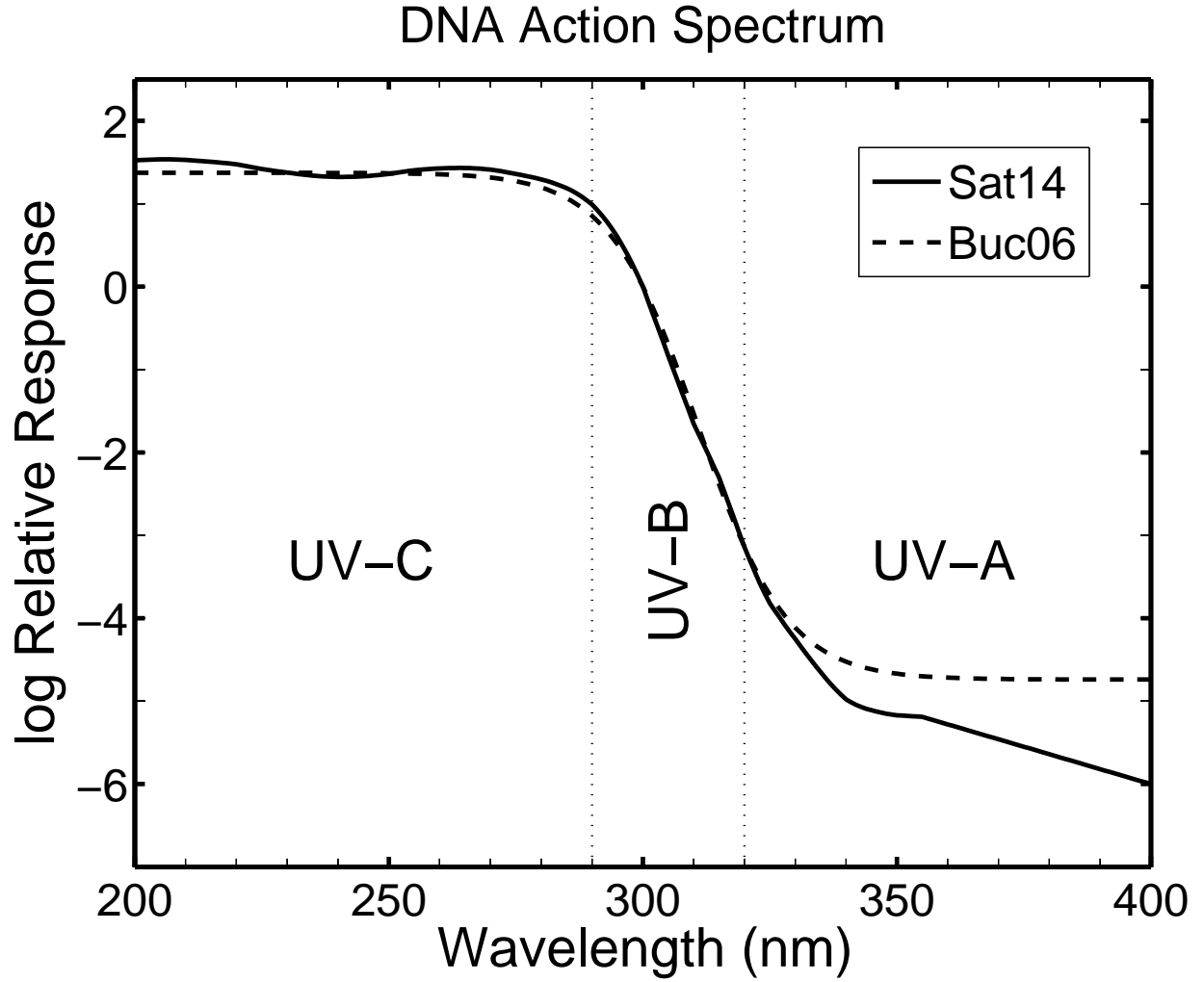


Fig. 4.— DNA action spectrum adopted from Paper I. The approximation previously used by Buccino, Lemarchand & Mauas (2006) is given for comparison.

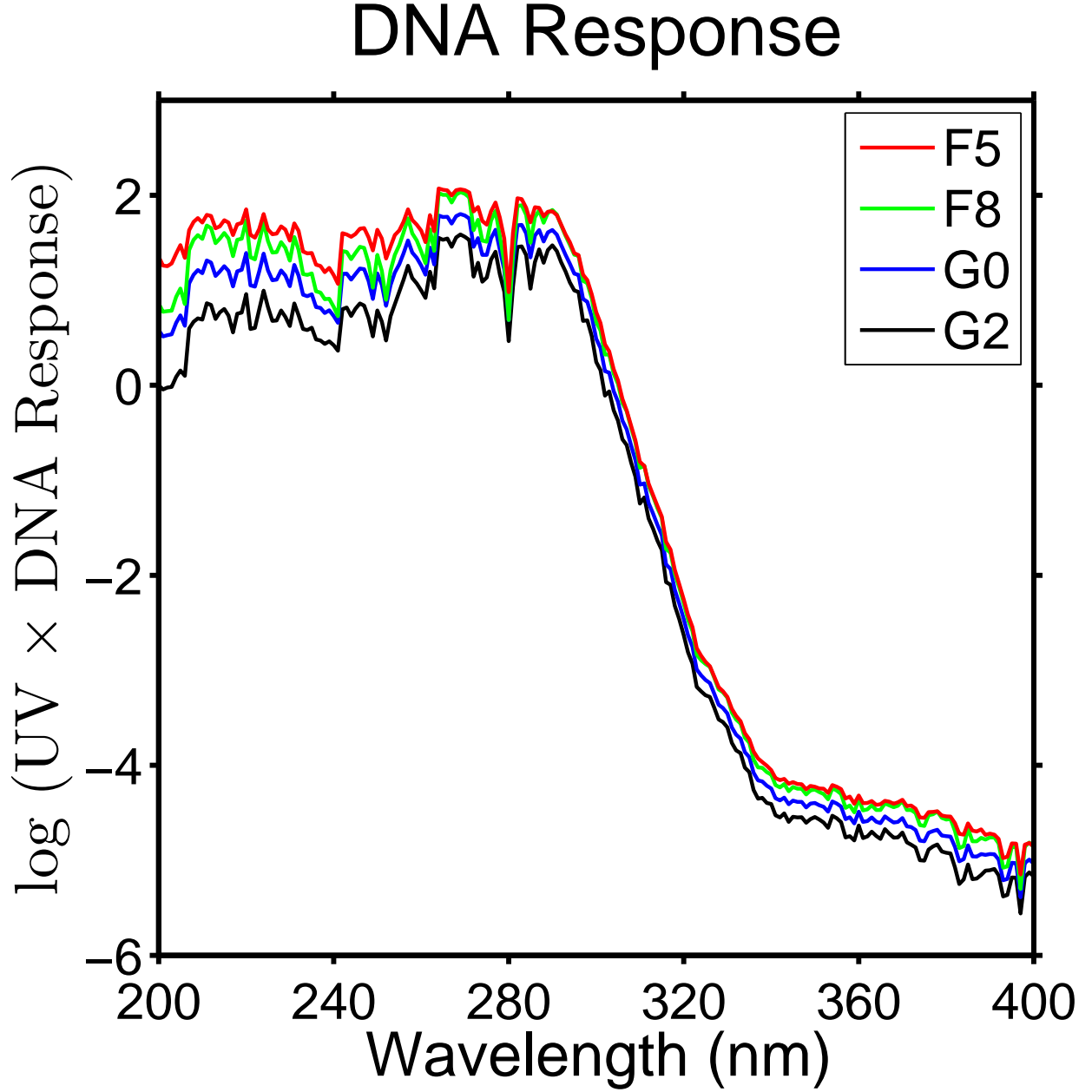


Fig. 5.— DNA response between wavelength of 200 and 400 nm pertaining to spectral irradiation by main-sequence stars between spectral type F5 and G2. The stellar spectra have been smoothed assuming a 1 nm running mean bandpass. Note that the  $y$ -axis has been normalized to unity for a G2 V star based on its PHOENIX spectrum.

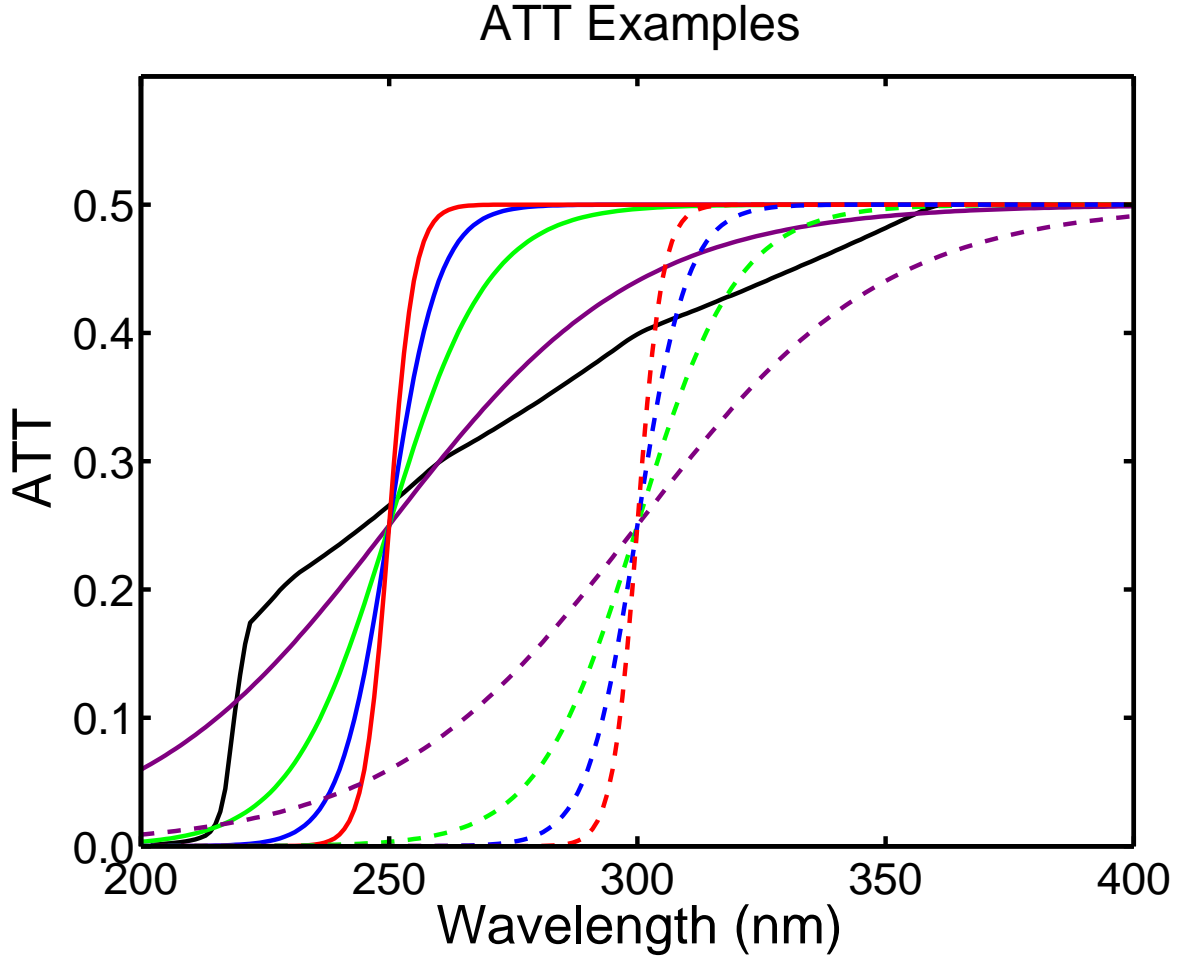


Fig. 6.— Examples of parameterized attention functions  $ATT$  defined through  $(A, B, C)$  with  $C = 0.5$  (see Eq. 3). The solid and dashed colored lines refer to  $B = 250$  and  $300$  nm, respectively. The colors red, blue, green, and purple refer to  $A = 0.20, 0.10, 0.05$ , and  $0.02$ , respectively. The heavy solid black line — that is fairly close to the solid purple line — indicates the case as deduced for Earth’s Archean eon (Cockell 2002). Note that the attention functions are not intended to fit data with the tentative exception of  $(0.02, 250, 0.5)$ .

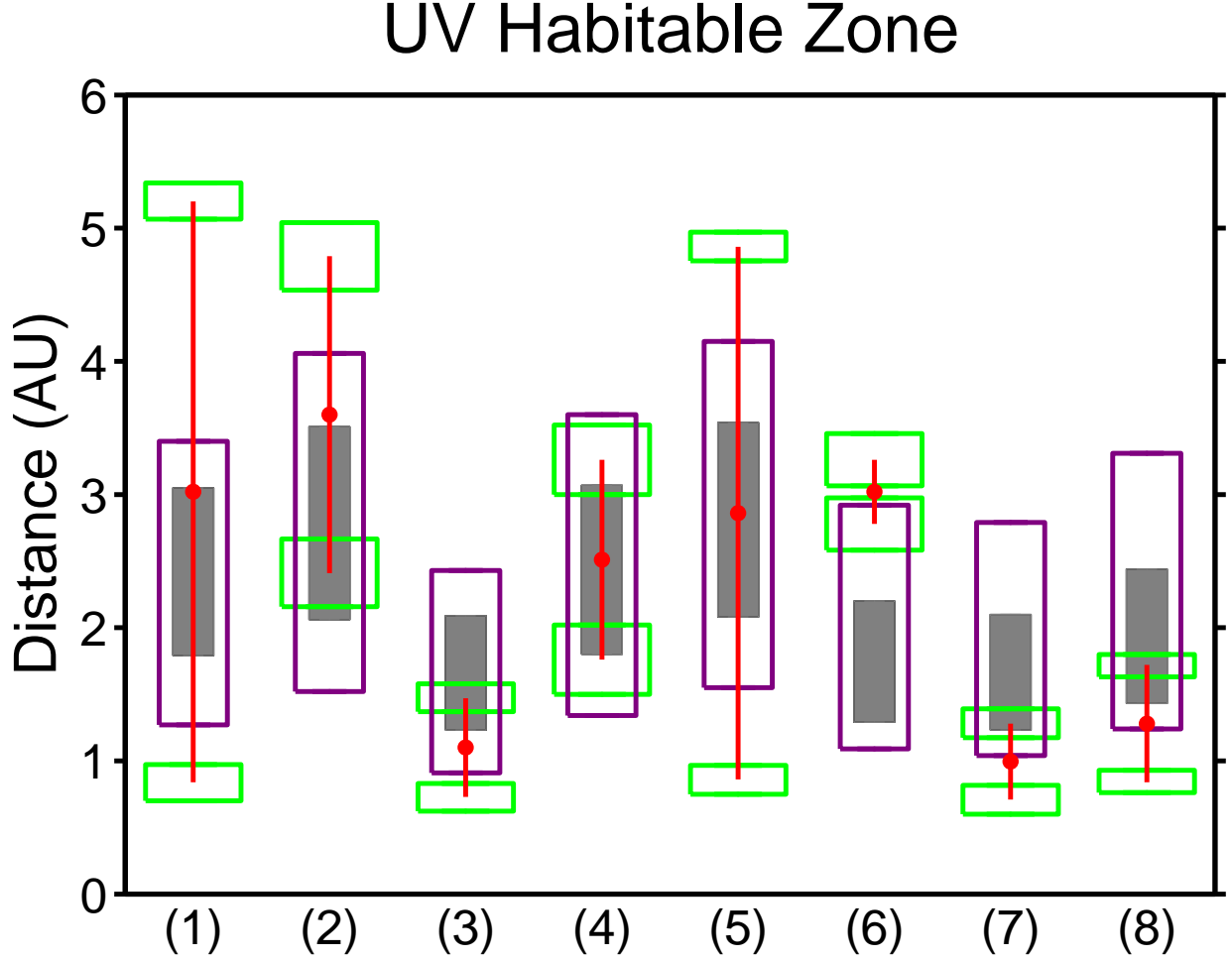


Fig. 7.— Depiction of stellar UV-HZs (purple), in comparison to the CLI-HZs, represented by the GHZs (medium gray), for the various star–planet systems of our study, indicated by (1) to (8). The positions of the giant planets are shown as red dots, whereas the ranges of the star–planet distances due to the eccentricity of the planetary orbits are shown as red lines. Additionally, for the planetary periaapsis and apoapsis positions, we depict the sizes of the Hill spheres (see Table 5) to convey the approximate maximal domains of possible exomoons.

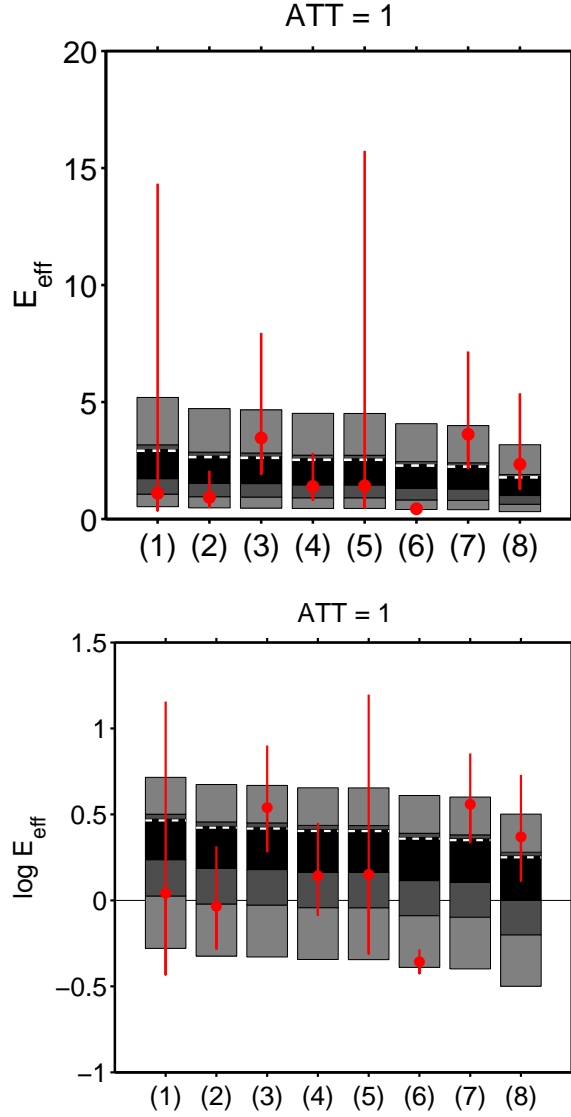


Fig. 8.— *Top:*  $E_{\text{eff}}$  for possible exomoons in reference to the stellar CLI-HZs. The CHZs, GHZs, and EHZs are indicated by dark gray, medium gray, and light gray colors. Earth-equivalent positions within the habitable zones are depicted by dashed lines. The target systems (see Table 1) indicated by (1) to (8). Additionally, we show the  $E_{\text{eff}}$  values for different positions as defined by the Jupiter-type planets. The ranges in  $E_{\text{eff}}$ , indicated by the red lines, are due to the eccentric planetary orbits. The red dots are depicting  $E_{\text{eff}}$ , when the planetary distance is given by its semimajor axis. *Bottom:* Replication of the top panel by choosing a logarithmic scale for enhanced representation.



Table 1. Target Stars

Star	Type	$T_{\text{eff}}$	$L_*$	$R_*$	$M_*$	Age	References
...	...	(K)	( $L_{\odot}$ )	( $R_{\odot}$ )	( $M_{\odot}$ )	(Gyr)	...
(1) HD 8673	F5 V $-27$ K	6413	3.60	1.54	1.312	2.52	1, 2 ( $T_{\text{eff}}$ ), 3 ( $R_*$ , $M_*$ , Age)
(2) HD 169830	F7 V $-14$ K	6266	4.69	1.84	1.4	2.3	4 ( $T_{\text{eff}}$ , Age), 5 ( $R_*$ , $M_*$ )
(3) HD 33564	F7 V $-30$ K	6250	1.66	1.1	1.25	3.0	6 ( $T_{\text{eff}}$ , $M_*$ , Age), 7 ( $R_*$ )
(4) $v$ And A	F8 V $+12$ K	6212	3.56	1.631	1.27	3.12	8 ( $T_{\text{eff}}$ ), 9 ( $R_*$ ), 10 ( $M_*$ ), 3 (Age)
(5) HD 86264	F8 V $+10$ K	6210	4.72	1.88	1.42	2.24	11
(6) HD 25171	F9 V $+35$ K	6160	1.80	1.18	1.09	4.0	12
(7) 30 Ari B	F9 V $+27$ K	6152	1.64	1.13	1.11	0.91	4 ( $T_{\text{eff}}$ , $M_*$ ), 13 ( $R_*$ , Age)
(8) HD 153950	G0 V $+26$ K	6076	2.20	1.34	1.12	4.3	14

Note. — For example, an expression such as F5 V  $-27$  K means that the stellar effective temperature is 27 K lower than that of a standard F5 V star noting that the standard  $T_{\text{eff}}$  values are those of the respective PHOENIX model. References: 1: Hartmann, Guenther & Hatzes (2010), 2: Fuhrmann (2008), 3: Takeda et al. (2007), 4: Nordström et al. (2004), 5: Fischer & Valenti (2005), 6: Galland et al. (2005), 7: Pasinetti Fracassini et al. (2001), 8: Santos, Israelian & Mayor (2004), 9: Baines et al. (2008), 10: Fuhrmann, Pfeiffer & Bernkopf (1998), 11: Fischer et al. (2009), 12: Moutou et al. (2011), 13: Guenther et al. (2009), and 14: Moutou et al. (2009). Note that  $L_*$  are calculated from  $T_{\text{eff}}$  and  $R_*$ .

Table 2. Climatological Habitable Zones

System ...	HZ-iE (AU)	HZ-iG (AU)	HZ-iC (AU)	Earth eqv. (AU)	HZ-oC (AU)	HZ-oG (AU)	HZ-oE (AU)
(1) HD 8673	1.39	1.79	1.84	1.85	2.41	3.05	4.37
(2) HD 169830	1.59	2.06	2.11	2.13	2.80	3.51	5.03
(3) HD 33564	0.95	1.23	1.25	1.27	1.67	2.09	2.99
(4) $\nu$ And A	1.39	1.80	1.84	1.86	2.45	3.07	4.39
(5) HD 86264	1.60	2.08	2.12	2.14	2.82	3.54	5.06
(6) HD 25171	0.99	1.29	1.31	1.32	1.75	2.20	3.13
(7) 30 Ari B	0.95	1.23	1.25	1.26	1.68	2.10	3.00
(8) HD 153950	1.10	1.43	1.45	1.47	1.95	2.44	3.48

Note. — See Glossary for information on acronyms. We also give the Earth-equivalent, i.e., homeothermic, distances.

Table 3. UV Habitable Zones

System ...	HZ-iUV (AU)	Earth eqv. (AU)	HZ-oUV (AU)
(1) HD 8673	1.27	1.85	3.40
(2) HD 169830	1.52	2.13	4.06
(3) HD 33564	0.91	1.27	2.43
(4) <i>v</i> And A	1.34	1.86	3.60
(5) HD 86264	1.55	2.14	4.15
(6) HD 25171	1.09	1.32	2.92
(7) 30 Ari B	1.04	1.26	2.79
(8) HD 153950	1.24	1.47	3.31

Note. — See Glossary for information on acronyms. We also give the Earth-equivalent, i.e., homeothermic, distances.

Table 4. Planetary Data

Planet ...	$M_p \sin i$ ( $M_J$ )	$a_p$ (AU)	$e_p$ ...	$a_p(1 - e_p)$ (AU)	$a_p(1 + e_p)$ (AU)	References ...
(1) HD 8673b	14.2	3.02	0.723	0.84	5.20	Hartmann, Guenther & Hatzes (2010)
(2) HD 169830c	4.04	3.6	0.33	2.41	4.79	Mayor et al. (2004)
(3) HD 33564b	9.1	1.1	0.34	0.73	1.47	Galland et al. (2005)
(4) $v$ And Ad	10.19	2.51	0.299	1.76	3.26	Curiel et al. (2011)
(5) HD 86264b	7.0	2.86	0.7	0.86	4.86	Fischer et al. (2009)
(6) HD 25171b	0.95	3.02	0.08	2.78	3.26	Moutou et al. (2011)
(7) 30 Ari Bb	9.88	0.995	0.289	0.71	1.28	Guenther et al. (2009)
(8) HD 153950b	2.73	1.28	0.34	0.84	1.72	Moutou et al. (2009)

Note. — See main text for original references. Also, for  $v$  And Ad,  $M_p$  is given here instead of the projected value.

Table 5. Hill Radius

Planet	$R_{\text{H}}$	$\tilde{R}_{\text{H}}$	$R_{\text{H}}/a_{\text{p}}$
...	(AU)	(AU)	...
(1) HD 8673b	0.14	0.49	0.045
(2) HD 169830c	0.25	0.38	0.071
(3) HD 33564b	0.10	0.16	0.095
(4) $\nu$ And Ad	0.26	0.37	0.104
(5) HD 86264b	0.11	0.36	0.038
(6) HD 25171b	0.20	0.21	0.065
(7) 30 Ari Bb	0.11	0.15	0.109
(8) HD 153950b	0.084	0.13	0.066

## A. Glossary

Acronym	Definition
ArcE	Archean Earth
AU	Astronomical Unit
CHZ	Conservative Habitable Zone
CLI-HZ	Climatological Habitable Zone
DNA	Deoxyribonucleic Acid
EHZ	Extended Habitable Zone
GHZ	General Habitable Zone
HZ-iC	Conservative Habitable Zone, inner limit
HZ-iE	Extended Habitable Zone, inner limit
HZ-iG	General Habitable Zone, inner limit
HZ-iUV	Ultraviolet Habitable Zone, inner limit
HZ-oC	Conservative Habitable Zone, outer limit
HZ-oE	Extended Habitable Zone, outer limit
HZ-oG	General Habitable Zone, outer limit
HZ-oUV	Ultraviolet Habitable Zone, outer limit
RNA	Ribonucleic Acid
RVEM	Recent Venus / Early Mars Habitable Zone
UV	Ultraviolet
UV-A	Ultraviolet, A-regime: 400–320 nm
UV-B	Ultraviolet, B-regime: 320–290 nm
UV-C	Ultraviolet, C-regime: 290–200 nm
UV-HZ	Ultraviolet Habitable Zone
PoM	Principle of Mediocrity
ZAMS	Zero-Age Main-Sequence